BILINGUAL PUBLISHING CO.
Pioneer of Global Academics Since 1984

Hydro Science & Marine Engineering
https://ojs.bilpublishing.com/index.php/hsme

ARTICLE

Stilling and its Aerodynamic Effects on Pan Evaporation

Qiang Liu [1,2] Sirui Yan [1,2] Liqiao Liang [3,4] Liya Su [1,2*]

1. Key Laboratory for Water and Sediment Sciences, Ministry of Education, School of Environment, Beijing Normal University, Beijing 100875, China
2. State Key Laboratory of Water Environment Simulation, School of Environment, Beijing Normal University, Beijing, 100875, China
3. Key Laboratory of Tibetan Environment Changes and Land Surface Processes, Institute of Tibetan Plateau Research, Chinese Academy of Sciences, Beijing 100101, China
4. Center for Excellence in Tibetan Plateau Earth Sciences, Chinese Academy of Sciences, Beijing 100101, China

ARTICLE INFO

Article history
Received: 7 August 2020
Accepted: 30 September 2020
Published Online: 30 October 2020

Keywords:
Wind speed
Pan evaporation
Stilling
PenPan model
Aerodynamic effect

ABSTRACT

Declines in wind speed (u) (termed as "stilling") has been reported in many regions of the world. To explore the temporal trends of u and its aerodynamic effects is vital to understand the changes in water resources. This study analyzed the changes of temporal trends for u and its aerodynamic effects using the data during 1959-2000 at 266 stations across China. The improved PenPan model was used to estimate pan evaporation (E_{pan}) and quantify the contribution of radiative and aerodynamic components (aerodynamic component separated into wind speed u, vapour pressure deficit D, and air temperature Ta). Climate factors include E_{pan} measured with the standard Chinese 20 cm diameter pan, u, Ta, relative humidity (rh) and sunshine hours (sh). The results showed: stilling occurred in most of stations (206 among 266) and 105 stations presented significant decreasing trends at 99% confidence level; stilling was the main cause for controlling the trends in E_{pan} in most part of China, especially in the west and north of China. The results indicated that decreasing trends in E_{pan} due to stilling would inevitably alter water resources, and should be put further investigation incorporation other factors.

1. Introduction

Declining rates of observed near-surface wind speed (u) (termed a "stilling", [1] are usually on the order of -0.010 m s^{-1} a^{-1} [2]. Stilling has been reported in many regions around the world, summarized by McVicar *et al*. [3] in Table 2, e.g., Australia [1], China [4], and North America [5]. Stilling alters the aerodynamic condition, which is the key factor in the fully physical-

**Corresponding Author:*
Liqiao Liang,
Key Laboratory of Tibetan Environment Changes and Land Surface Processes, Institute of Tibetan Plateau Research, Chinese Academy of Sciences, Beijing 100101, China;
Center for Excellence in Tibetan Plateau Earth Sciences, Chinese Academy of Sciences, Beijing 100101, China;
Email: liangliqiao@itpcas.ac.cn;
Liya Su,
Key Laboratory for Water and Sediment Sciences, Ministry of Education, School of Environment, Beijing Normal University, Beijing 100875, China;
State Key Laboratory of Water Environment Simulation, School of Environment, Beijing Normal University, Beijing, 100875, China;
Email: liya@bnu.edu.cn

DOI: https://doi.org/10.30564/hsme.v2i2.2266

ly-based models to assess the evaporation demand [6,7], such as potential evaporation (E_p), references evapotranspiration (ET_0) and pan evaporation (E_{pan}). Due to its simplicity and cost effectiveness, E_{pan} has been widely used to reflect the evaporation demand of the atmosphere when estimating terrestrial evaporation [8] and crop water requirement [9].

The "evaporation paradox" phenomenon, that is decline trend in pan evaporation with increasing trend in air temperature, has drawn great attention to explore causes for changes in pan evaporation and its application for global hydrological cycle [2, 10]. Different from the empirical method used to estimate pan evaporation [11-15], Rotstayn *et al*. [16] combined the works of Linacre [17] and Thom *et al*. [18] to develop a steady state pan evaporation model for a US Class A pan called the "PenPan model, which has been used to assess the cause of pan evaporation (e.g., Roderick *et al*., [1]). Improved by Yang and Yang [19], PenPan model also was used to simulate the changes in pan evaporation for the standard Chinese 20 cm diameter pan (D20 pan). According to Yang and Yang [19] and Xie *et al*. [20], the declines in u were the main causes for changes in pan evaporation in most parts of China. As pointed out by Thom *et al* [18], vapour transfer function- $f_q(u)$ depends not only on wind speed but also on the difference between surface temperature for water and air temperature [18]. Thom *et al*., (1981) [18] deduced the wind function f_q(u) (unit: mm d^{-1} mb^{-1}) as:

$$f_q(u) = 0.12 \times (1 + 1.35u) \tag{1}$$

where, u (m s^{-1}) is the mean wind speed at two meters above the ground. Yang and Yang (2012) [19] deduced the $f_q(u)$ using the data in Beijing stations as:

$$f_q(u) = 5.4 \times (1 + 0.40u) \tag{2}$$

Vapour transfer function should be an attractive approach to establish a physical model and derive its differential to analyze the attribution of changes in E_{pan} [19]. Consequently, the objectives of the present study are: (*i*) to explore the temporal trends for u across China, and explain where can found the stilling; and (*ii*) to improve the PenPan model using vapour transfer function, and to explain aerodynamic effects of declines of u. To address these objectives the remainder of this paper is structured as followed: section 2 presented the physical model for analyzing the aerodynamic effects of stilling; section 3 explained the materials and method; section 4 explored the temporal trends for u; and section 5 gave the aerodynamic effects of the stilling.

2. Materials and Method

2.1 Assessing the Aerodynamic Effects of Stilling Using PenPan Model

The PenPan model is based on Penman's combination equation, using Linacre [17] and Thom *et al*. [18] models to describe the radiative and aerodynamic components [16], respectively. The PenPan model can be represented as:

$$E_p = E_{p,R} + E_{P,A} = \left(\frac{s}{s+a\gamma}\frac{R_n}{\lambda}\right) + \left(\frac{a\gamma}{s+a\gamma}\frac{f_q(u)D}{\lambda}\right) \tag{3}$$

where, s (P_a K^{-1}) is the change in saturation vapour pressure (e_s, Pa) with temperature evaluated at the air temperature (T_a, K) two meters above the ground, R_n (W m^{-2}) is the net radiation on the pan, λ (J kg^{-1}) is the latent heat of vaporization, α is the ratio of effective surface area for heat and vapour transfer (α=5 for D20 pan) [19], γ (~67 Pa K^{-1}) is the psychrometric constant, D (= e_s-e_a, Pa) is the vapour pressure deficit at two meters, and f_q *(u)* (mm d^{-1} mb^{-1}) is the vapour transfer function.

Following Roderick *et al*. [1], changes in pan evaporation can result from radiative and aerodynamic components and be given by differentiating equation,

$$\frac{dE_p}{dt} = \frac{dE_{p,R}}{dt} + \frac{dE_{p,A}}{dt} \tag{4}$$

Then $dE_{p,A}/dt$ is partitioned into three components, denoted U*, D* and T* for changes in u, D and T_a respectively. The components are defined by,

$$\frac{dE_{p,A}}{dt} \approx \frac{dE_{p,R}}{du}\frac{du}{dt} + \frac{dE_{p,R}}{du}\frac{dD}{dt} + \frac{dE_{p,R}}{dT_a}\frac{dT_a}{dt} = U^* + D^* + T^* \tag{5}$$

As u trends present different patterns, we get $f_q(u)$~u from 266 stations using 1959-1969 monthly data. According to the $f_q(u)$, the improved PenPan model based on Yang and Yang's [19] equation is used to assess the aerodynamic effects of u changes across China.

2.2 Meteorological Data

In order to test the temporal trends for u and its aerodynamic effects on E_{pan}, data were collected from China Meteorological Administration (CMA), including monthly E_{pan}, u, T_a, relative humidity (rh) and sunshine hours (sh) from 266 stations across China (Figure 1). Considering the data integrity and continuity, 266 stations were selected to do this work during 1959-2000 (Figure 1).

 DOI: https://doi.org/10.30564/hsme.v2i2.2266

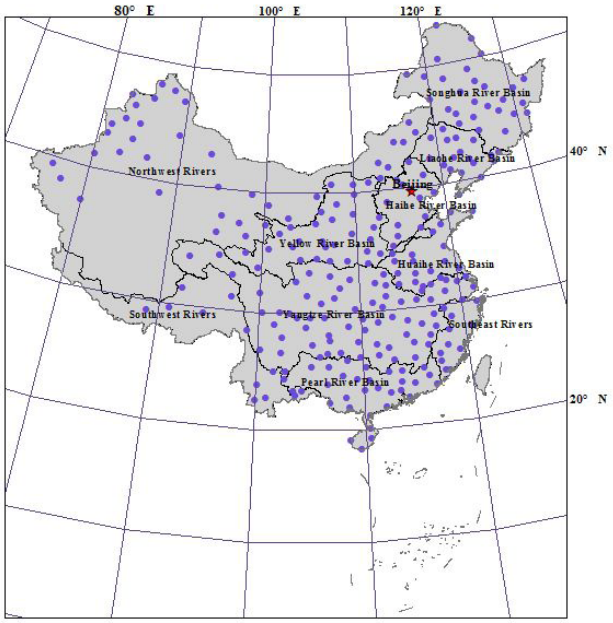

Figure 1. Locations of meteorological stations across China used in this study. Furthermore, basins also presented in the Figure, such as Songhua River Basin (SRB), Liaohe River Basin (LRB), Haihe River Basin (HHRB), Yellow River Basin (YRB), Huaihe River Basin (HuaiRB), Yangtze River Basin (YzRB), Pearl River Basin (PRB), Southwest Rivers Basin (SWRB), Northwest Rivers Basin (NWRB) and Southeast Rivers Basin (SERB)

Due to that radiation component was not observed at most stations, net radiation (R_n) was calculated at monthly scale using the equation as follows:

$$R_n = (1-\alpha_p)R_{sp} + R_{l,in} - R_{l,out} \quad , \tag{6}$$

where, R_{sp} is the incoming shortwave radiation on a pan, $R_{l,in}$ is the incoming longwave radiation, $R_{l,out}$ is the outgoing longwave radiation, estimated by assuming that the pan is a black body radiating at T_a, α_p is constant (=0.14).

$$R_{sp} = \left[f_{dir}P_{rad} + 2.0*(1-f_{dir}) + 2.0*A_s\right]R_s \quad , \tag{7}$$

where R_s is the downward solar irradiance at the surface, f_{dir} is the fraction of R_s that is direct, A_s (=0.23) is the albedo of the ground surrounding the pan, and P_{rad} is the pan radiation factor, which accounts for the extra direct irradiance intercepted by the walls of the pan when the sun is not directly overhead.

$$R_{l,in} = \sigma T_a^4 (1-(0.34-0.14\sqrt{e_a/1000}) \cdot (1.35R_s/(R_o(0.75+2\times10^{-5}z))-0.35)) \quad , \tag{8}$$

where σ is Stefan-Boltzmann constant (4.903*10^{-9} MJ m^{-2} K^{-4}day^{-1}), e_a is the actual vapor pressure (P_a), R_o is solar radiation on the top of the atmosphere, and z (m) is the station elevation [9].

3. Results

3.1 The Trends Pattern of Wind Speed Over China

As showed in Figure 2, stilling phenomena has experienced across China. The average u trend of -0.012 m s^{-1} a^{-1} was in agreement with results presented for other mid-latitude site. Furthermore, temporal trends for u in mid-latitude basins (i.e. HuaiRB: -0.023 m s^{-1} a^{-1}; NWRB: -0.022 m s^{-1} a^{-1}) presented obviously downward trends, followed by north basins (i.e. SHRB: -0.015 m s^{-1} a^{-1}, LHRB: -0.013 m s^{-1} a^{-1}) and south regions (i.e. YzRB: -0.008 m s^{-1} a^{-1}, PRB: -0.008 and SWRB: -0.001 m s^{-1} a^{-1}).

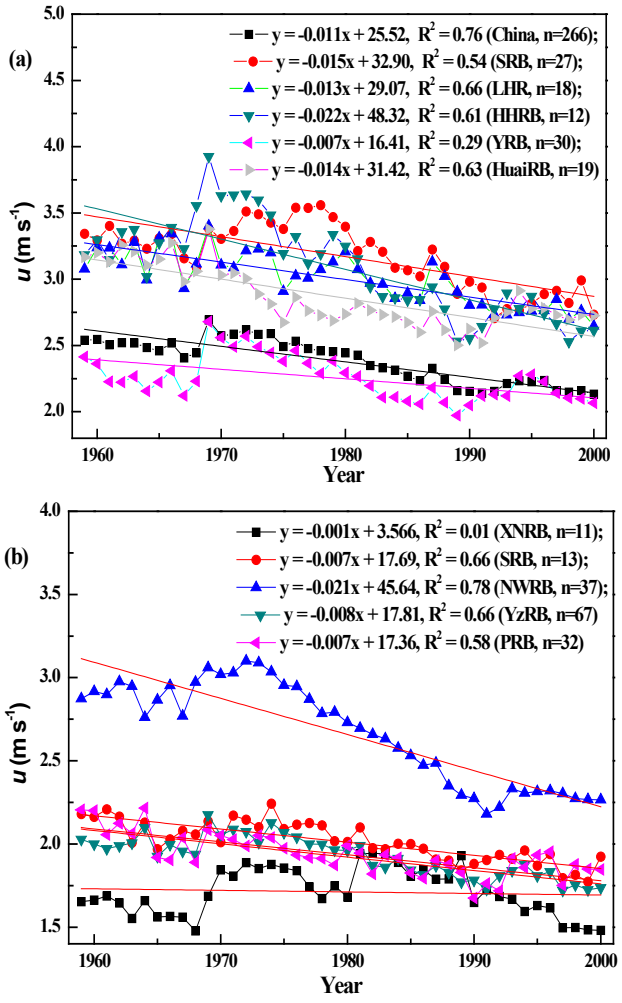

Figure 2. The temporal trend of u in different regions of China. Furthermore, number of stations used in different basin also presented in the bracket

DOI: https://doi.org/10.30564/hsme.v2i2.2266

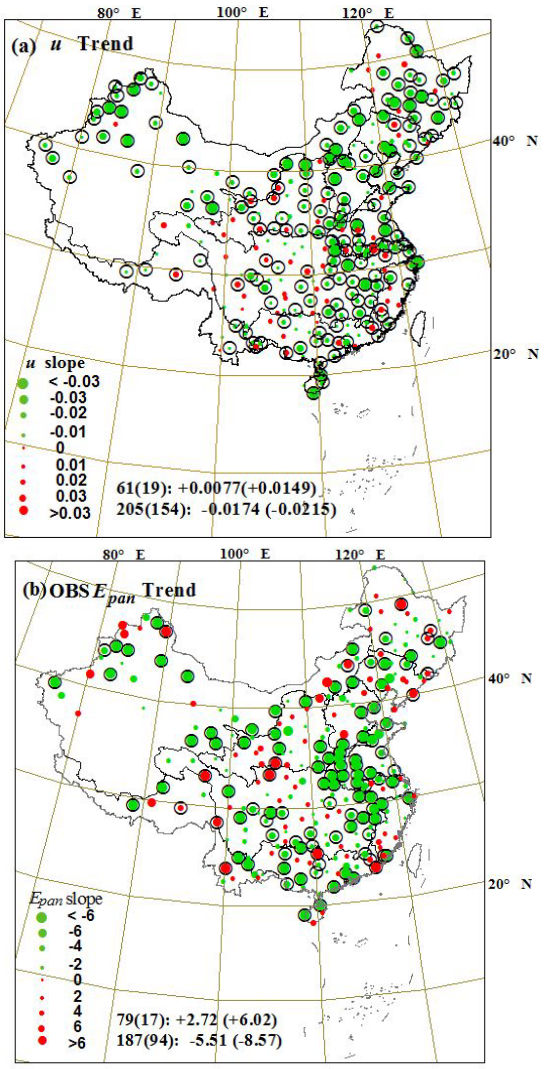

Figure 3. Temporal trends for u (a) and E_{pan} (b) across China during 1959-2000. If the trend is significant ($P < 0.01$), a ring is placed around the dot; units is m $s^{-1}a^{-1}$ for u and mm a^{-2} for E_{pan}. The values located in the bottom of plot are interpreted as follows. The first line shows in order from left to right: (1) the number of stations with positive u and E_{pan} trends; (2) in parenthesis the number of stations with significant ($P < 0.01$) positive u and E_{pan} trends; (3) the u and E_{pan} trend (units = mm a^{-2}) calculated for all stations with positive trends; and (4) in parenthesis the u and E_{pan} trend (units = mm a^{-2}) calculated for all stations with significant ($P < 0.01$) positive u and E_{pan} trends. The second line presents the same four statistics except for stations exhibiting negative u and E_{pan} trends

The temporal trends for u (Figure 3a) presented that: (1) most of stations (205 among 266) presented negative trends with an average slope of -0.0174 m s^{-1} a^{-1}, while only 61 stations showed positive trends with an average slope of 0.0077 m s^{-1} a^{-1}; (2) especially, there were 154 stations showing significant negative trends at 99% confidence level with an average slope of -0.0215 mm a^{-2}, and only 19 stations showed significant positive trends at 99% confident level with an average slope of 0.0149 mm a^{-2}. Stilling in u altered the E_{pan} trends. As showed in Figure 3b, E_{pan} presented similar trends with the changes in u trends: (1) most of stations (187 among 266) showed negative trends, while only 79 stations presented positive trends; (2) the numbers of stations showing negative and positive significant trends at 99% confident level were 94 and 17, respectively.

3.2 Aerodynamic Effects of Stilling on the E_{pan}

Using data from 266 stations during 1959-1969, $f_q(u)$~u equation can be recalibrated from equation (9):

$$f_q(u) = 9.58 \times (1+0.40u) \quad R^2 = 0.27. \tag{9}$$

The equation was used to simulate the E_{pan} across China. The calculated E_{pan} was compared with observed E_{pan} in 266 stations (Figure 4). Compared with results using Yang and Yang's equation [19] (y=2.54+1.62x, R^2=0.91, RMSE=107 mm mth^{-1}), the agreement between improved modeled and observed E_{pan} at 266 stations (y=8.73+0.99x, R^2=0.94, RMSE=23 mm mth^{-1}) was excellent.

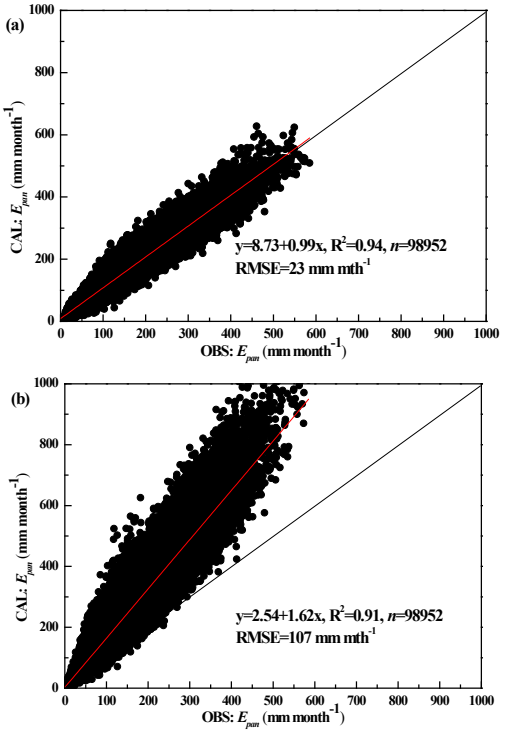

Figure 4. Comparison of the observed (OBS) and calculated (CLAC) monthly E_{pan} during 1970-2000 from 266 stations across China. (a) using $f_q(u)$ from Eq. (9), (b) using $f_q(u)$ from Eq. (2) for Yang and Yang[19]'s equation. Best fit regression and 1:1 line were also showed. Furthermore, the R^2 and RMSE were showed for the 98952 data between observed and calculated monthly E_{pan}.

 DOI: https://doi.org/10.30564/hsme.v2i2.2266

Following the method provided by Roderick *et al*. [1], we separated the E_{pan} rate into radiative and aerodynamic components, and then aerodynamic component was separated into three individual components (U*, D* and T*) (showed in Table 1 and Figure 5). The results showed: (1) changes in aerodynamic component controlled the trends in E_{pan} (Figure 5.c), and changes in u contributed majority of changes in E_{pan} trends (Figure 5d); (2) the changes in D (Figure 5e) and T_a (Figure 5f) attributed a minor changes in E_{pan} trends; (3) as expected, E_{pan} trends and its radiative and aerodynamic components showed spatial variations, i.e, u contributed negative effects in E_{pan} trends, especially in NWRB and middle and lower regions of YRB and Upper reaches of HuaiRB. The downward trends in u resulted in two regions showing large decreasing trends in E_{pan}, NWRB, and the regions in Middle-lower regions YRB and upper HuaiRB (Table 1 and Figure 5), that consistent with the trends in OBS E_{pan} (Figure 3b); and (4) as showed in Table 1 and Figure 5, u and T_a played negative effect in $E_{pan,A}$ trends, while changes in D contributed a positive effect in $E_{pan,A}$ trends, which resulted in an increasing E_{pan} trends in YRB, PRB, SWRB and SERB and opposite trends showed in others basins (Table 1).

Table 1. Observed (OBS) and model-calculated (CACL) trends in E_{pan} rate (dE_{pan}/dt, in mm a^{-2}) in different regions of China for 1959-2000

Regions	OBS	CAL-C=Rad+Aero	Rad	Aero	Aero Partition		
	dE_{pan}/dt	dE_{pan}/dt	$dE_{pan,R}/dt$	$dE_{pan,A}/dt$	U^*	D*	T*
China	-3.06	-1.11	-0.06	-1.06	-2.51	1.69	-0.33
SRB	-1.21	0.36	0.39	-0.03	-2.39	2.84	-0.42
LRB	-0.89	-0.30	0.17	-0.47	-2.76	2.90	-0.44
HHRB	-4.41	-1.45	0.21	-1.66	-4.79	3.53	-0.53
YRB	-2.82	1.13	0.30	0.83	-1.80	2.80	-0.44
HuaiRB	-7.48	-2.25	-0.44	-1.81	-2.74	0.63	-0.25
YzRB	-3.00	-1.61	-0.51	-1.10	-1.49	0.24	-0.11
PRB	-3.10	0.77	-0.35	1.12	-1.59	2.97	-0.23
NWRB	-4.38	-5.42	0.41	-5.83	-5.86	0.83	-0.64
SWRB	0.02	1.13	0.44	0.69	-0.43	1.50	-0.28
SERB	-1.83	-0.23	-0.57	0.33	-1.34	1.79	-0.15

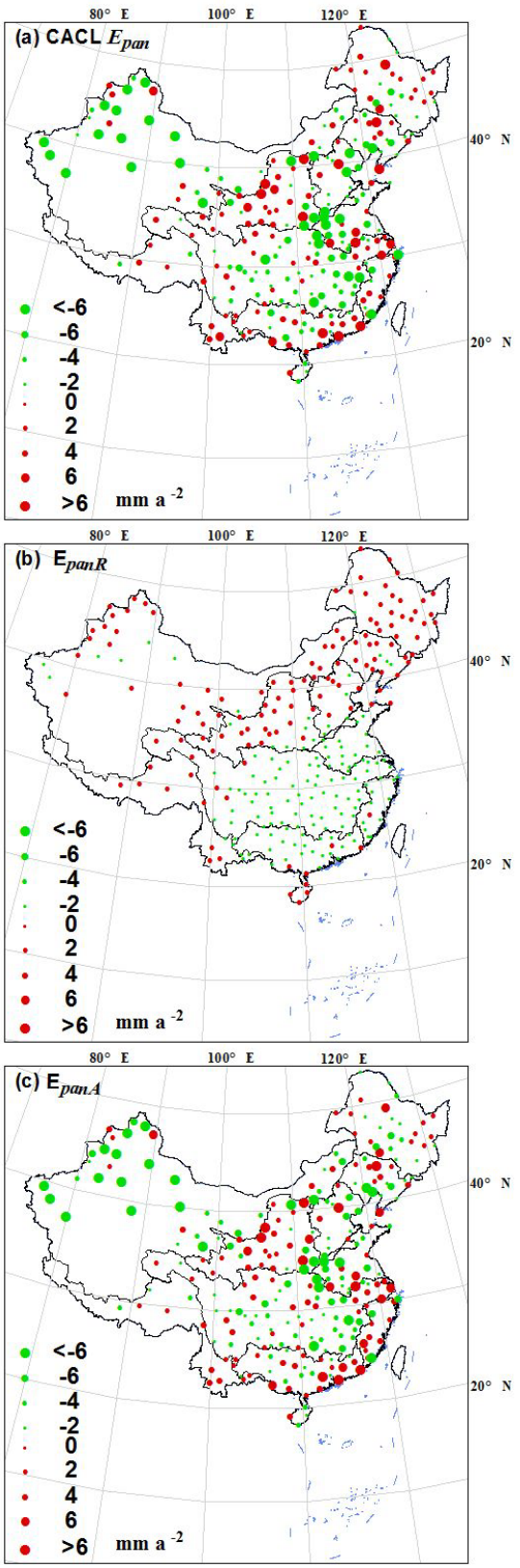

DOI: https://doi.org/10.30564/hsme.v2i2.2266

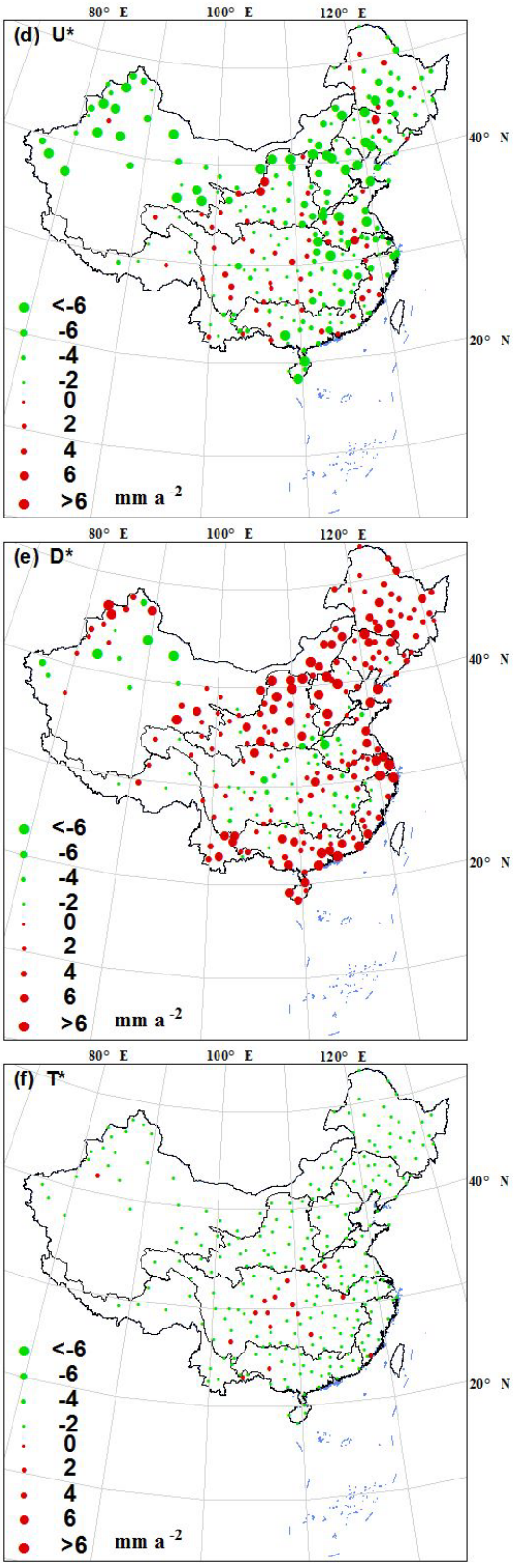

Figure 5. Trends in simulated pan evaporation and its components at 266 stations for the period 1959-2000. (a) Calculated E_{pan} rate. (b) Radiative component of pan evaporation ($E_{pan,R}$) rate. (c) Aerodynamic component of pan evaporation ($E_{pan,A}$) rate. The trends in the aerodynamic component are further partitioned into the change due to (d) U*, (e) D*, and (f) T*. The change in each panel, averaged across all 266 stations is (a) -1.11 mm a^{-2}, (b) -0.06 mm a^{-2}, (c) -1.06 mm a^{-2}, (d) -2.51 mm a^{-2}, (e) +1.69 mm a^{-2}, and (f) -0.33 mm a^{-2}

4. Discussion

4.1 Changes in Temporal Trends in Wind Speed

As addressed in Figure 3a, wind speed presented stilling phenomenon at 77% (205/266) stations across China with an average temporal trends at -0.011 m s^{-1} a^{-1}. Across China, in agreement with our study, downward trends in *u* [4,19-23] have been widely reported. Similar decreasing trends from -0.004 m s^{-1} a^{-1} to -0.017 m s^{-1} a^{-1} in near-surface *u* have been widely observed across the globe over the last 30-50 years (i.e., since ~1960s to ~1980s) for a range of mid-latitude regions (McVicar *et al*. [3] their Table 4). As showed in Figure 2 and Figure 3a, large declines were found in northern China, while central and south-central China have the least change in *u*. Except for Tibetan Plateau, the results are consistent with report by Guo *et al*. [4]. The precise cause of the stilling is uncertain [5], the explained for this phenomena lies in two aspects: (1) changes of land surface roughness (e.g., increasing vegetation cover and urbanization); and (2) influences resulting from the climate changes (e.g., weakening of the East Asian winter and summer monsoons). E.g., Guo *et al*. [4] stratified China 652-station database into rural and large-urban cases, and deduced that urbanization strengthened *u*. While Li *et al*. [24], using 12 stations to study the greater Beijing Area during 1960-2008, suggested that urbanization contributed one-fifth of the regional mean declining trend about −0.05 m s^{-1} $(10\ a)^{-1}$, and also noted that changes in strong winds (i.e., wind extremes and winter winds) are influenced by large-scale climatic change. As pointed by Chen *et al*. [25], the warm and cold Arctic Oscillation and El Nino-Southern Oscillation phases have significant influence on probability distribution of wind speeds, and thus internal climate variability is a major source of both interannual and long-term variability. The weakening of the East Asian winter and summer monsoons is the cause for the distinct decreases of wind speed over the whole China [21,23]. Furthermore, sharp step in *u* correspond well with the positive and negative phases of the interdecadal Pacific oscillation [22].

 DOI: https://doi.org/10.30564/hsme.v2i2.2266

4.2 Aerodynamic Effects of the Stilling in Wind Speed

Changes in E_{pan} caused by aerodynamics changes are larger than that caused by radiative components in most of regions of China (8 of 10) (Table 1). Declines in *u* play an important role in controlling the changes in $E_{pan,A}$ than that resulting from vapour pressure deficit and air temperature (Showed in Figure 5 and Table 1). Consistent with our results, changes in *u* is the main cause for changes in $E_{p,}$ [26], E_{pan} [19] and ET_0 [27] in China due to its significant downward trend and high sensitivity. Stilling reduced E_{pan} [1, 28, 29], ET_0 [30] and ET_p [31] rate, and has been regarded as important factor in explaining E_{pan} paradox [1,3], which means it is important to consider all four primary meteorological variables (being *u*, atmospheric humidity, radiation and T_a) [3]. As *u* exerting greater influence on energy-limited water yielding catchments than water-limited ones, it is vital to incorporate other factors to assess the impacts of evaporation demand on long term water resources [3]. Changes in *u* combining with other meteorological variables led to larger changes in E_{pan} in water-limited regions in northwest and North China (i.e., NWRB, SRB, LRB and HHRB) than that in energy-limited regions in South and central China (i.e., YzRB, PRB, SWRB and SERB) (showed in Table 1 and Figure 5). That indicated it is really hard to define the influence for the changes in *u* on water resources when involving the actual evapotranspiration and streamflow in different regions. As pointed by McVicar *et al*. [32], impacts of stilling on actual evapotranspiration and streamflow are situation dependent.

5. Conclusion

Changes of *u* during 1959-2000 from 266 stations across China presented an average decreasing trend of -0.012 m s^{-1} a^{-1}. There are 154 (among 205 negative trends stations) stations presenting significant decreasing trends at 99% confidence level while only 19 (among 61 positive trends stations) stations presenting significant increasing trends at 99% confidence level. Stilling in China was similar to the decrease reported over other terrestrial surface, which can explain the evaporation paradox.

Using a fully physical model (the improved Penpan model), we assessed the E_{pan} trends, and then quantified the aerodynamic effects resulting from the *U**, *D** and *T**. Stilling was the main cause for controlling the trends in E_{pan} in most of part of China, especially in the west and north of China. Our results suggest that stilling can reduce evaporation demand, and inevitably alter the water resources especially in the energy-limited regions, which should be put to further investigation incorporating with other factors.

Acknowledgments

This research was supported by the National Key Basic Research and Development Project (No. 2017YFC0404505, 2016YFC0500402), and the National Natural Science Foundation of China (No. 51579008), and Beijing Municipal Science and Technology Project (No: 217300011). Thanks to the National Meteorological Information Center, China Meteorological Administration, for offering the meteorological data.

References

[1] Roderick, M.L., Rotstayn, L.D., Farquhar, G.D., Hobbins, M.T. On the attribution of changing pan evaporation. Geophysical Research Letters, 2007, 34: L17403.
DOI: 10.1029/2007GL031166

[2] McVicar, T.R., Van Niel, T.G., Roderick, M.L., Li, L.T., Mo, X.G., Zimmermann, N.E., Schmatz, D.R. Observational evidence from two mountainous regions that near-surface wind speeds are declining more rapidly at higher elevations than lower elevations: 1960-2006. Geophysical Research Letters, 2010, 37: L06402.
DOI: 10.1029/2009GL042255

[3] McVicar, T.R., Roderick, M.L., Donohue, R.J., Li, L.T., Van Niel, T.G., Thomas, A., Grieser, J., Jhajharia, D., Himri, Y., Mahowald, N.M., Mescherskaya, A.V., Kruger, A.C., Rehman, S., Dinpashoh, Y. Global review and synthesis of trends in observed terrestrial near-surface wind speeds: Implications for evaporation. Journal of Hydrology, 2012a, 416-417: 182-205.

[4] Guo, H., Xu, M., Hu, Q. Changes in near-surface wind speed in China: 1969-2005. International Journal of Climatology, 2011, 31(3): 349-358.

[5] Vautard, R., Cattiaux, J., Yiou, P., Thépaut, J.-N., Ciais, P. Northern hemisphere atmospheric stilling partly attributed to increased surface roughness. Nature Geoscience, 2010, 3 (11): 756-761.

[6] Lim, W.H., Roderick, M.L., Hobbins, M.T., Wong, S.C., Groeneveld, P.J., Sun, F.B., Farquhar, G.D. The aerodynamics of pan evaporation. Agricultural and Forest Meteorology, 2012, 152: 31-43.

[7] Lim, W.H., Roderick, M.L., Farquhar, G.D. A mathematical model of pan evaporation under steady state conditions. Journal of Hydrology, 2016, 540: 641-658.

[8] Kohler, M.A., Noredenson, T.J., Fox, W.E. Evaporation from Pans and Lakes. US Weather Bureau Research Paper 38. US Weather Bureau, Washington, D.C, 1955.

DOI: https://doi.org/10.30564/hsme.v2i2.2266

[9] Allen, R.G., Pereira, L.S., Raes, D., Smith, M. Crop evapotranspiration-Guidelines for computing crop water requirements. FAO Irrigation and Drainage Paper 56, Rome, Italy, 1998.

[10] Roderick, M.L., Farquhar, G.D. The cause of decreased pan evaporation over the past 50 years. Science, 2002, 298: 1410-1411.
DOI:10.1126/science.1075390-a

[11] Qian, Y., Kaiser, D.P., Leung, L.R., Xu, M. More frequent cloud-free sky and less surface solar radiation in China from 1955 to 2000. Geophysical Research Letters, 2006, 33: L01812.
DOI: 10.1029/2005GL024586

[12] Shen, Y.J., Liu, C.M., Liu, M., Zeng, Y., Tian, C.Y. Change in pan evaporation over the past 50 years in the arid region of China. Hydrological Processes, 2010, 24(2): 225-231.

[13] Liu, X.M., Luo, Y.Z., Zhang, D., Zhang, M.H., Liu, C.M. Recent changes in panevaporation dynamics in China. Geophysical Research Letters, 2011a, 38: L13404.
DOI: 10.1029/ 2011GL047929

[14] Liu, X.M., Zheng, H.X., Zhang, M.H., Liu, C.M.. Identification of dominant climate factor for pan evaporation trend in the Tibetan Plateau. Journal of Geographical Sciences, 2011b, 21(4): 594-608.

[15] Zhang, Q., Qi, T.Y., Li, J.F., Singh, V.P., Wang, Z.Z. Spatiotemporal variations of pan evaporation in China during 1960-2005: changing patterns and causes. International Journal of Climatology, 2015, 35: 903-912.

[16] Rotstayn, L.D., Roderick, M.L., Farquhar, G.D. A simple pan-evaporation model for analysis of climate simulations: Evaluation over Australia. Geophysical Research Letters, 2006, 33: L17715.
DOI: 10.1029/2006GL027114

[17] Linacre, E.T. Estimating United States Class-A pan evaporation from few climate data. Water International, 1994, 19(1): 5-14.

[18] Thom, A. S., Thony, J. L., Vauclin, M. On the proper employment of evaporation pans and atmometers in estimating potential transpiration, Quarterly Journal of the Royal Meteorological Society, 1981, 107: 711-736.

[19] Yang, H., Yang, D. Climatic factors influencing changing pan evaporation across China from 1961 to 2001. Journal of Hydrology, 2012, 414-415:184-193.

[20] Xie, H., Zhu, X., Yuan, D.Y. Pan evaporation modelling and changing attribution analysis on the Tibetan Plateau (1970-2012). Hydrological Processes, 2015, 29: 2164-2177.

[21] Xu, M., Chang, C.P., Fu, C.B., Qi, Y., Robock, A., Robinson, D., Zhang, H.M. Steady decline of East Asian monsoon winds, 1969-2000: evidence from direct ground measurements of wind speed. Journal of Geophysical Research-Atmospheres , 2006c, 111: D24111.
DOI: 10.1029/2006JD007337

[22] Fu, G.B., Yu, J.J., Zhang, Y.C., Hu, S.S., Ouyang, R.L., Liu, W.B. Temporal variation of wind speed in China for 1961-2007. Theoretical and Applied Climatology, 2011, 104(3-4): 313-324.

[23] Jiang, Y., Luo, Y., Zhao, Z.C. Maximum wind speed changes over China. Acta Meteorologica Sinica,, 2013, 27(1): 63-74.

[24] Li, Z., Yan, Z.W., Tu, K., Liu, W.D., Wang, Y.C. Changes in wind speed and extremes in Beijing during 1960-2008 based on homogenized observations. Advances Atmospheric Sciences, 2011, 28(2): 408-420.

[25] Chen, L., Li, D., Pryor, S.C. Wind speed trends over China: quantifying the magnitude and assessing causality. International Journal of Climatology, 2013, 33(11): 2579-2590.

[26] Zhang, C., Liu, F., Shen, Y. Attribution analysis of changing pan evaporation in the Qianghai-Tibetan Plateau, China. International Journal of Climatology, 2018, 38 (Suppl. 1): e1032-e1043.

[27] Yin, Y. H., Wu, S. H., Chen, G., Dai, E. F. Attribution analyses of potential evapotranspiration changes in China since the 1960s. Theoretical and Applied Climatology, 2010, 101(1-2): 19-28.

[28] Rayner, D.P. Wind run Changes: Dominant factor affecting pan evaporation trends in Australia. Journal of Climate, 2007, 20(14): 3379-3394.

[29] Roderick, M.L., Hobbins, M.T., Farquhar, G.D. Pan evaporation trends and the terrestrial water balance, I. Principles and observations. Geography Compass 3/2, , 2009: 746-760.

[30] Liu, Q., Yang, Z.F., Cui, B.S., Sun, T. The temporal trends of reference evapotranspiration and its sensitivity to key meteorological variables in the Yellow River Basin, China. Hydrological Processes, 2010, 24: 2171-2181.

[31] Donohue, R.J., McVicar, T.R., Roderick, M.L.. Assessing the ability of potential evaporation formulations to capture the dynamics in evaporative demand within a changing climate. Journal of Hydrology, 2010, 386: 186-197.

[32] McVicar, T.R., Roderick, M.L., Donohue, R.J., Van Niel, T.G. Less bluster ahead? Ecohydrological implications of global trends of terrestrial near-surface wind speeds. Ecohydrology, 2012b, 5(4): 381-388.

 DOI: https://doi.org/10.30564/hsme.v2i2.2266